Astron. Astrophys. 326, 300–304 (1997)

ASTRONOMY AND ASTROPHYSICS

Observation of inhomogeneities in the wind of the luminous red supergiant μ Cephei*

N. Mauron

GRAAL, CC072, CNRS / Université de Montpellier II, Place Eugène Bataillon, F-34095 Montpellier Cedex 05, France
(mauron@merlin.graal.univ-montp2.fr)

Received 20 January 1997 / Accepted 22 April 1997

Abstract. Long-slit spectrograms of the circumstellar envelope of the M2Ia luminous supergiant μ Cep are presented. This cool wind emits fluorescent KI 7665-7699Å lines and has been resolved along two north-south slits, located 5″ and 10″ west from the star. The angular resolution was ∼0.6″. A low spectral resolution of 40 km s^{-1}, i.e. about the emission line width, was used, permitting to be sensitive and to detect KI emission up to ∼60″ from the star. The distributions of KI line emission along these two strips display bumps and breaks, which suggest that important inhomogeneities exist in the flow. Their apparent size is about 1″-3″, corresponding to ∼1-3 10^{16} cm for a distance of 830pc. The data suggest that density contrasts of an order of magnitude occur in the wind at the above scales, although interpretation of the KI line intensity is subject to uncertainties concerning ionization and line transfer in a clumpy medium. Assuming that these inhomogeneities are in fact arc-like shells ejected episodically by the star, a typical mass-loss timescale of ∼1000 years is derived.

Key words: stars: mass loss – stars: circumstellar matter – stars: μ Cep – supergiants

1. Introduction

The structure of circumstellar envelopes around cool late-type stars (asymptotic giant branch stars and red supergiants) is of interest with regard to both mass loss mechanism and circumstellar physico-chemistry. Recent observations, in particular those made at high angular resolution, point to a process which, at a given time, may not be spherical, and bipolar in some cases (see for example Kahane & Jura 1996, or Plez & Lambert 1994 and references therein). Other techniques which probe a much larger extent of the envelopes with low resolution such as the IRAS or ISO far-infrared images, suggest that the mass loss rate can strongly vary (e.g. Waters et al. 1994, Izumiura et al. 1996, Olofsson et al. 1996). Episodic mass loss has also been invoked in the past because of the presence of discrete velocity components in circumstellar optical absorption lines (Ridgway 1981).

The case of massive red supergiants (RSGs) is important because they evolve into Wolf-Rayet stars or/and Type II supernovae (SN). After SN explosion, optical emission is produced by interaction of the expanding SN gas with the cool wind. In their model of this emission, Chevalier & Fransson (1994) assume a smooth r^{-2} RSG wind density, and this hypothesis should be tested as far as possible, especially regarding the effect of clumpiness. An equatorial density enhancement of RSG winds is also possible: it has been invoked both concerning the geometry SN 1987A circumstellar matter (Blondin & Lundqvist 1993, Meyer 1997), and concerning the elongated shape of some Wolf-Rayet bubbles (Brighenti & D'Ercole 1996). Whether this geometry is general in optical and dusty RSG, whether it is linked with rotation, magnetic field, binarity or other processes, are still open questions.

In this context, we present high angular resolution observations of the wind of μ Cep. This M2Ia supergiant is one of the most luminous RSG: if one adopts a distance of 830pc (Humphreys 1978), its parameters are: L ∼4 10^5 $L_\odot$, T_{eff}=3560K, R = 1600$R_\odot$ (Jura & Kleinmann 1990, di Benedetto 1993). The main sequence progenitor mass should be ∼35$M_\odot$. There are also indications that this star is single, with at least no hot main sequence companion like α Sco or VV Cep, since no characteristic emission lines or ultraviolet excess are detected (Rogers et al. 1983), and since its large envelope is essentially neutral (Mauron et al. 1986, Guilain & Mauron 1996).

In order to probe circumstellar matter over a large extent (for studying mass loss history) and with a high angular resolution (for structure), long-slit spectroscopy in the KI $\lambda 7665-7699$ lines was used. A low spectral resolution of ∼40 km s^{-1} was chosen in order to have a relatively high sensitivity, at the ex-

Send offprint requests to: N. Mauron

* Based on observations made at the 3.6-m Canada-France-Hawaii telescope, operated by the National Research Council of Canada, the Centre National de la Recherche Scientifique of France, and the University of Hawaii

pense of kinematic information. In the following, Sect. 2 describes the observations and the data reductions. The results are given and analysed in Sect. 3. Discussion is in Sect. 4, and the main conclusions of this work are summarized in Sect. 5.

2. Observations and reductions

The observations were carried out on 1992 July 5 with the CFH 3.6-m telescope and the Herzberg spectrograph. The detector was a thick blue-coated PHX 512x512 CCD chip having a quantum efficiency of 30% at 8000Å, a read-out noise of 8e, a gain of 1.8 e ADU^{-1} and a pixel size of 20μm. The spectrograph was used with a 0.75″-wide and 131″-long slit, a grating of 830 lines mm^{-1} working in the first order, providing a dispersion of 0.97 Å pixel^{-1}. Along the slit, the 20μm pixel represented 0.611″. The sky was clear and the seeing was about 0.5″.

We made two off-star spectra, with exposure times of 1000 and 2000s, and with the slit oriented north-south and located at $\sim$5″ and $\sim$10″ west of the star. There is unfortunately a significant uncertainty in the accuracy of these offsets for two reasons: first, after positionning the slit, we noted that switching the guiding system on could occasionally induce a supplementary shift of $\pm$0.5″ ; secondly, the telescope position was erroneously not recorded in the headers of the FITS files during observations of μ Cep. This was corrected later on in the run for other objects, but we realized that requested offsets of e.g. 3.0″ were in fact between 1.5″ and 4.5″ . Consequently, the $\sim$5″ and $\sim$10″ offsets are known within 1.5″ at best.

We also took on-star spectra through a neutral filter of density 2, and one such spectrum was done with opened slit, in order to calibrate the shell brightnesses on the stellar flux. The latter, measured on the average "continuum" beside the 7700Å absorption line, gave 5.7 10^5 ADU s^{-1} Å^{-1}. Bias and flat-field exposures were also secured in order to clean on-star and off-star frames in a standard way.

The bulk of off-star signal along the slit comes from scattered stellar light and from an east-west diffraction spike, but KI shell emission is already visible on uncleaned frames. For each given position along the slit, one gets a linear spectrum along a CCD row, showing sky lines, shell emission lines and scattered light. The latter was substracted by scaling the on-star spectrum (see Mauron & Caux 1992). The result is a net spectrum with the KI lines spread over 2-3 pixels, and numerous sky emission lines. The flux integrated over each KI line was measured for every such spectrum, finally providing line brightness distributions along the slit, displayed in Fig.1. In the following, the height on slit is noted h, which is null nearest to the star and positive to north; the radial distance to the star is $r = (r_0^2{+}h^2)^{1/2}$, with offsets r_0 beeing 5″ or 10″ , except otherwise specified.

Several comments are in order concerning these distributions. First, the λ7665 line may suffer from telluric O_2 absorption; in addition, a faint sky line on the blue side of λ7665 prevented us to measure its intensity at very faint levels. Nevertheless the λ7665 distributions are a useful check of the λ7699 ones. Secondly, at very low brightnesses, we had to make averages over 2 to 5 CCD rows, which degrades the angular resolution to 1.2″ or even to 3″ along the slit, as can be seen on Fig. 1. Finally, relative uncertainties (1 σ) on line fluxes are estimated to be about $\pm$5% at high levels and about $\pm$30% at low ones, i.e. $\pm$0.02 and $\pm$0.1 in log scale, respectively.

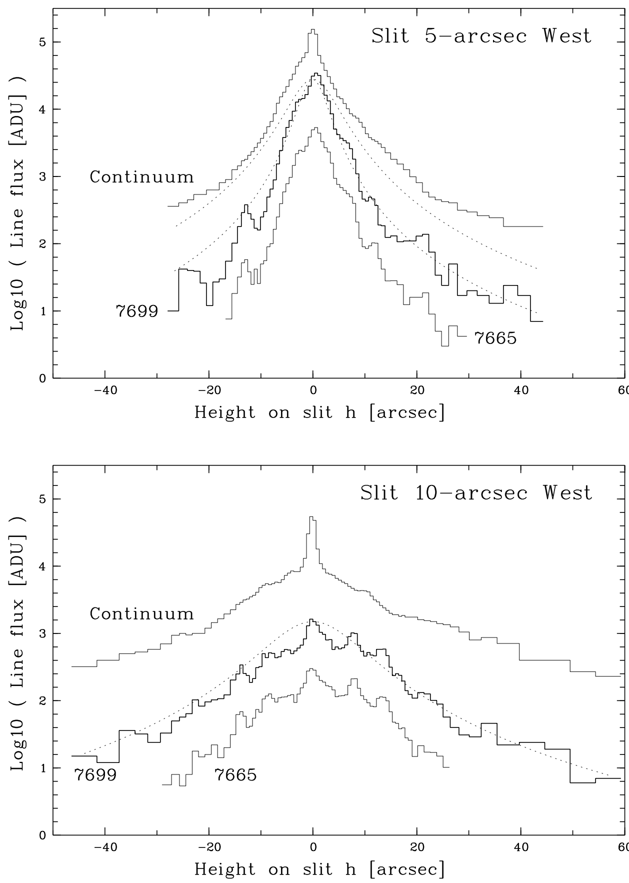

Fig. 1. Distribution of the KI line emission along the slits at 5″ and 10″ west of μ Cep (binned curves labelled 7699 and 7665; for clarity, the 7665 curve has been shifted down by 0.7 in log). The distribution of continuum scattered light is also shown for comparison. The dotted lines represent: -a/ in the top plot, two r^{-3} distributions with $r = (h^2 + r_0^2)^{1/2}$, r_0 beeing 5″ and 3″ (upper and lower curve, respectively); -b/ in the bottom plot an r^{-3} distribution with r_0=10″ (see text). The coordinates are linear-log.

3. Results and analysis

3.1. Reliability of the data

Fig. 1 shows important bumps and breaks in the KI distributions, and, as noted by the referee, one might ask "are they real"? We claim they are, for the following reasons:

- Examination of sky emission lines and flat-fields show the intrumental sensitivity to be smooth along the slit, with a large scale amplitude of at most $\pm$10%. This effect is corrected and cannot produce the bumps.
- On the 5″ slit frame, the lines are very strong and seen in emission well above continuum for $|h|$ <10″ , even on not flat-fielded frames. We checked that the very steep declines at

h = +5″ and h = +10″ are real, and much larger than the stellar continuum gradients. The bump at $h = -13''$ is also visible before and after any cleaning.

- One can note however that the continuum also presents small bumps. Its distribution cannot be perfectly fitted by a smooth radial law (ignoring the diffraction spike), and there are significant north-south asymmetries. We believe that this is attributable in part to the telescope scattered halo itself, in qualitative agreement with coronographic imaging experiments at CFH by Walker et al. (1994). One can also think about parasite reflections inside the spectrograph since the spike and line emissions are very intense in the middle of the slit. In principle reflections might create at any h some artificial KI bumps. However, this effect may be reasonably excluded by the fact that we do not find any correlation, neither in position nor in amplitude, between continuum and line spatial fluctuations.

- the best slope fitting the continuum is near -2, in agreement with the seeing profile of King (1971), whereas we find for KI lines a best slope of about -3, or more negative (see below), which further supports the correctness of data reductions.

3.2. The general shape of KI line distributions

The λ7699 or λ7665 distributions of Fig.1 can first be compared with a simple model distribution in which one assumes a circumstellar density of KI atoms running as r^{-2}, isotropic illumination from the star and optically thin line scattering. These assumptions imply a brightness distribution $I \propto r^{-3}$, i.e. $I \propto (r_0^2 + h^2)^{3/2}$, with r_0 being the slit offset. Fig.1 shows that such a model can reasonably fit the *general shape* of the observed KI distribution along the 10″ slit. In the case of the 5″ slit, choosing r_0=3″ considerably improves the fit, and as explained in Sect. 2, such a 3″ value is not completely excluded. If however the offset was really 5″ , an excess of emission by a factor of about 5-10 is suggested for $|h| < 10''$, possibly due to a density enhancement ∼5″ west of the star. In any case, substantial discrepancies, much larger than experimental errors, remain between any smooth model and the observed bumpy distributions.

3.3. Discrete shells

Many interpretations can be proposed to explain the bumps. A first possibility to consider is extinction by small interstellar KI clouds located on the line of sight to the envelope. Structures with appropriate scales (800-4000AU, i.e. 1″-5″ at 800pc) are known to exist in the diffuse interstellar medium (Watson & Meyer 1996), but due to a favorable stellar radial velocity, not much KI absorption is expected to occur (Mauron & Le Borgne 1989, appendix B; Mauron & Querci 1990).

One could also think that bumps reveal in fact the patchiness that would result from superposition on the line of sight of numerous small circumstellar clumps randomly located in the whole volume of the envelope. This structure has been proposed by Olofsson et al. (1996) for the detached envelopes of carbon stars, and this possibility cannot be ruled out by the present data.

In our opinion, it is however more tempting to imagine the bumps and breaks as due to limb brightening by several more or less spherical bubbles separated by low density gaps. Such a structure is qualitatively consistent with other observations of μ Cep: discrete circumstellar components are seen in the KI and CO absorption lines (Bernat 1981); at least 2 shells are suggested by Fabry-Perot images made in the NaI lines (Mauron et al. 1986, Mauron & Le Borgne 1989), by polarization measurements (Le Borgne & Mauron 1989), and by far-infrared scans (Hawkins 1993). Arc-like structures or detached shells are also present in many winds of very different stars, for example the Cepheid RS Pup (Havlen 1972, Deasy 1988), IRC+10216 (Crabtree et al. 1987), the post-AGB CLR 2688 (Sahai et al. 1995).

After adopting this kind of geometry and still assuming single scattering of KI line photons, it is possible to get a first (and admittedly coarse) approximation of the KI density distribution $n(r)$, by fitting the intensity distributions with the relation:

$$I_r \propto \int \; n((r^2 + l^2)^{1/2}) \; (r^2 + l^2)^{-1} \; dl \qquad (1).$$

Fig. 2 shows such a fit for the 10″ strip, for which we considered separately the north and south parts. We have assumed that within any individual shell, the density obeys a r^{-2} law, as if the star had experienced successive periods of steady mass-loss, with alternatively high and low mass loss rates. From this analysis, we find that the widths of high mass loss shells would be typically 1″-3″ , whereas the widths of low mass loss shells appear to be statistically larger (3″-10″). The KI density contrast between these shells can reach a factor of ∼30. Such a large value comes in part from the observations, but also from our assumption of spherical symmetry in applying Eq. (1). This is because any given dense shell produces a significant intensity for a line of sight passing just inside its inner radius, and this limits the amount of density for the next inner tenuous shell. But, as can be seen in Figs. 1 and 2, north-south symmetry is not well respected.

4. Discussion

The first inescapable conclusion of the above analysis is that the envelope of μ Cep (M2Ia) is not smooth. Even if we drop the assumption of shells, the observed distributions suggest typical clump sizes of one to several arcseconds, and large density variations. This is significantly more inhomogeneous than one could have thought from previous findings. The wind of Betelgeuse (M2Iab), which is possibly very similar, has been studied with long-slit spectra or maps in the KI lines by Bernat et al. (1978), Honeycutt et al. (1980) and Mauron et al. (1984), but has not revealed such a structure. This may be due in part to improvement of observational techniques: the data of this work are deep, have good photometric precision, high dynamic range and subarcsecond angular resolution. Another possibility is that, as suggested by its numerous circumstellar absorption components, the wind of μ Cep is intrinsically more inhomogeneous than Betelgeuse's one.

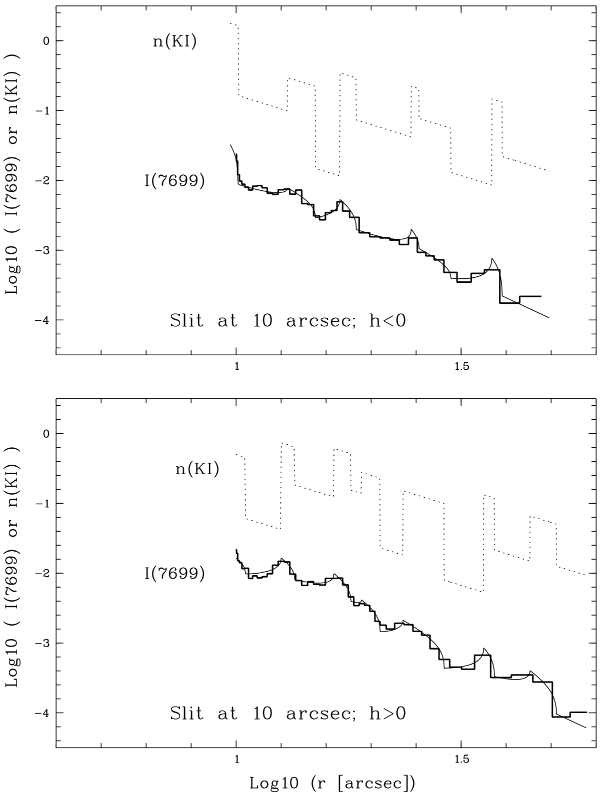

Fig. 2. Fits of the KI intensity distributions with several shells. The observed data are in thick stepped lines, and the model intensity superposed in thin lines. The KI density distributions are in dotted lines. Only relative values of intensities and densities are significant. The scales are log-log.

Physically, the specificities of the KI tracer and induced uncertainties are important to consider, regarding the analysis done in Sect. 3: the question is how fluctuations of KI line intensity are linked to those of hydrogen density, and this involves line radiative transfer and KI fractional ionization. Concerning the line opacity, reliable measured values of the ratio 7665/7699 range from 0.7 to 1 ($\pm$0.05) at $\sim5''$ cut, and from 0.9 to 1.1 at $10''$. Telluric O_2 absorption at $\lambda7665$ certainly lowers the true values: assuming that the 7665 line is gaussian, 2Å wide and centered on $v_{star,helio}$=19.3 km s^{-1}(see the spectra in Mauron and Guilain 1995), this absorption can be shown to be 20-30% at most in the present data (O_2 line profiles are given in Chaffee & White 1982). So the real 7665/7699 ratioes should be between 0.9 and 1.40. This is in favour of a significant optical depth, $\tau\sim1$ or larger at $\sim$5-$10''$.

Concerning the ionization fraction γ_{KI}=n_{KI}/n_K and the link to n_H, local equilibrium between photoionization and recombination was adopted by Mauron & Caux (1992) and by Guilain & Mauron (1996), following on this point the analysis of Glassgold & Huggins (1986) and their equation (5.1). Recently, the validity of equilibrium has been questioned by Gustafsson et al. (1997). These authors find that assuming γ_{KI}=1 yields mass-loss rates in good agreement with values derived from CO for three carbon stars. However, it is premature, as they admit, to reject the equilibrium approximation on the basis of these stars because large uncertainties exist on their ultraviolet fluxes or other parameters involved in equilibrium calculations, and on CO-based mass loss rates as well. On the other hand, the assumption γ_{KI}=1 and their related equation (6) cannot be valid in general: when applied to warmer stars like α Ori or α Her with much surer information on UV fluxes and mass-loss rates, one finds too small mass loss rates (3 10^{-8} and 7 10^{-10} $M_\odot$ yr^{-1} for these two stars, respectively, i.e. about 100 times too low), and this supports γ_{KI} <<1 on average in their winds. To summarize, a correct estimation of γ_{KI} has to be done in all cases to interpret KI emission, and this is not easy even when equilibrium is assumed, since local values of T, n_e and ionizing UV field are required. This applies *a fortiori* in the present case, where the obvious inhomogeneity should be taken into account. At this stage, we cannot decide whether fluctuations δn_{KI} scale as δn_H or as $(\delta n_H)^2$, or in between.

Consequently, we consider that the shell characteristics derived in Sect.3 may be somewhat biased by this KI tracer: for instance, the hydrogen density contrast between dense and tenuous shells may be lower than the obtained high value (i.e. up to $\sim$ 30), but it would still reach at least $\sim$5 if $\delta n_{KI}\propto(\delta n_H)^2$.

Finally, in the hypothesis that discrete arc-like shells are really present and due to episodic ejections from the star, one can derive a characteristic time-scale of outbursts: with typical angular separations between shells in the $3''-10''$ range, we find 1200 years (after taking d = 830 pc and v = 20 km s^{-1}). This timescale is much larger than the pulsation periods of 2.4 and 13.3 years found in μ Cep's photometric variations (Mantegazza 1982). It also cannot be related to thermal pulses, since this star is a true red supergiant. This intriguing situation was already pointed out by Ridgway (1981) from a statistical analysis of absorption circumstellar lines, and is not changed by observations which angularly resolve the envelopes, like in the present work, or like in the case of IRC+10216 (Crabtree et al. 1987) or CRL 2688 (Sahai et al. 1995, Deguchi 1996), for which ejection timescales of 200-400 years are derived.

5. Conclusions

In this paper, we presented KI long-slit spectroscopy of the envelope of μ Cep, made with slits $\sim5''$ and $10''$ west of the star. Accurate and deep photometry of KI line emission along two $0.7''$ x $100''$ strips, with an angular resolution of $\sim0.5''$, have been obtained. The wind has been detected up to $\sim60''$ from the star. These observations show that important inhomogeneities exist in the wind of this massive red supergiant, with typical sizes of $\sim1''$-$3''$, or $\sim$1-3 10^{16}cm. It is possible that these inhomogeneities are due to episodic mass loss with a typical timescale of $\sim$1000 years.

Further observations, especially imagery, are needed in order to ascertain the possible circularity of these inhomogeneities, and a possible density enhancement at $5''$ west of the star. Since the size of these inhomogeneities is also not very different from our resolution, investigating the structure at even smaller scales should also be attempted. Observing envelopes at high resolution with various tracers like fluorescent KI and NaI, CO emission, and scattered light by dust should also be useful to reduce uncertainties specific to the interpretation of each species, and finally obtain a better characterization of their density distribution, clumpiness and kinematics.

Acknowledgements. I would like to thank Drs E. Caux, J. Glaspey, D. Salmon and the telescope operators for help during observations, and Dr. Th. Le Bertre for comments. Useful remarks by the referee Dr A.E. Glassgold are also greatly acknowledged by the author. This work has made use of SIMBAD, operated at the Centre de Données Stellaires (Strasbourg, France), and has been supported in part by the "Groupes de Recherche du CNRS": "Physico-Chimie des Molécules et Grains Interstellaires", and "Milieux Circumstellaires".

References

Bernat A.P., 1981, ApJ 246, 184
Bernat A.P., Honeycutt R.K., Kephart J.E. et al., 1978, ApJ 219, 532
Blondin J.M., Lundqvist P., 1993, ApJ 405, 337
Brighenti F., D'Ercole A., 1997, MNRAS 285, 387
Chaffee F.H., White R.E., 1982, ApJSS 50, 169
Chevalier R.A., Fransson C., 1994, ApJ 420, 268
Crabtree D.R., Mc Laren R.A., Christian C.A., 1987, in Late Stages of Stellar Evolution, Kwok S., Pottasch, S.R. (eds.), Reidel, Dordrecht, p. 145
Deasy H.P., 1988, MNRAS 231, 673
Deguchi S., 1996 Molecular envelopes of young and proto-planetary nebulae. In: " Planetary Nebulae" IAU Symp. 180, Groningen
Di Benedetto G.P., 1993, A&A 270, 315
Glassgold A.E., Huggins P.J., 1986, ApJ 306, 605
Guilain Ch., Mauron N., 1996, A&A 314, 585
Gustafsson B., Eriksson K., et al., 1997, A&A 318, 535
Havlen R.J., 1972, A&A 16, 252
Hawkins G.W., Smith B.J., Harvey P., 1993, Far-Infrared Imaging of Red Giants and Supergiants with the Kuiper Aiborne Observatory. In: Schwarz H.E. (ed.) ESO Conferences and Workshops Proc. N^o 46, Mass Loss on the AGB and Beyond, ESO, Garching, p. 203
Honeycutt R.K., Bernat A.P., Kephart J.E. et al.: 1980, ApJ 239, 565
Humphreys R., 1978, ApJSS 38, 309
Izumiura H., Hashomoto O., Kawara K. et al., 1996, A&A 315, L221
Jura M., Kleinmann S.G., 1990, ApJSS 73, 769
Kahane C., Jura M., 1996, A&A 310, 952
Le Borgne J.-F., Mauron N., 1989, A&A 210, 198
King I.R., 1971, PASP 83, 199
Mantegazza L., 1982, A&A 111, 295
Mauron N., Fort B., Querci F., et al., 1984, A&A 130, 341
Mauron N., Cailloux M., Tilloles P. et al., 1986 A&A 165, L9
Mauron N., Caux E., 1992, A&A 265, 711
Mauron N., Guilain Ch., 1995, A&A 298, 869
Mauron N., Le Borgne J.-F., 1989, Observations of the Circumstellar Environment of Two Red Supergiant. In: Delache P., Laloe S., Magnan Ch. (eds.) Modeling The Stellar Environment: How and Why. Editions Frontières, Gif-sur-Yvette, p. 279
Mauron N., Querci F., 1990, A&ASS 86, 513
Meyer F., 1997, MNRAS 285, L11
Olofsson H., 1996, The neutral envelopes around AGB and post-AGB objects: their structure and evolution. In: Wings B. (ed.) Proc. IAU Symp. 177, The Carbon Star Phenomenon.
Olofsson H., Bergman P., Eriksson K. et al., 1996, A&A 311, 587
Plez B., Lambert D.L., 1994, ApJ 425, L101
Ridgway S.T., 1981, Timescale of possible episodic behavior in mass loss from cool stars. In. Iben I., Renzini A. (eds) Physical Processes in Red Giants, Reidel, Dordrecht, p. 305
Rogers C., Martin D.G., Crabtree D.R., 1983, ApJ 272,175
Sahai R., Trauger J.T., Evans, R.W., 1995, BAAS 27, 1344; (image in HST press release STScI-PRC96-05)
Walker G., Walker A., Racine R. et al., 1994, PASP 106, 356
Waters L.B.F.M., Loup C., Kester C., et al. 1994, A&A 281, L1
Watson J.K., Meyer D.M., 1996, ApJ 473, L127

This article was processed by the author using Springer-Verlag LaTeX A&A style file *L-AA* version 3.